Small-particle composites. II. Nonlinear optical properties

Vladimir M. Shalaev,* E. Y. Poliakov, and V. A. Markel†
Department of Physics, New Mexico State University, Las Cruces, New Mexico 88003
(Received 17 March 1995; revised manuscript received 22 June 1995)

Strong fluctuations of local fields may result in very large optical nonlinearities in small-particle composites. Enhancement associated with particle clustering is found for a number of optical processes, including four-wave mixing (FWM), third-harmonic generation (THG), Raman scattering, and nonlinear refraction and absorption in Kerr media. Field fluctuations and optical nonlinear susceptibilities are especially large in fractal clusters. The enhancement of optical processes is expressed in terms of the resonant linear absorption by collective dipolar eigenmodes in a cluster, and quality factors, q, of the modes ($q \gg 1$). It is shown that the susceptibility of a composite material consisting of random small-particle clusters is proportional to q^3 for Raman scattering and the Kerr optical nonlinearity, and to q^4 and q^6 for THG and FWM, respectively. For all of these processes, a spectral dependence of the effective susceptibility is found. Broad-scale numerical simulations of the optical response in small-particle composites are performed to complement the theory. The simulations are in reasonable agreement with available experimental data.

I. INTRODUCTION

Nonlinear electrical and optical properties of nanostructured composites have attracted much attention in recent years.[1–14] Composite materials can have much larger nonlinear susceptibilities at zero and finite frequencies than those of ordinary bulk materials. The enhancement of the nonlinear optical response in composites is due to strong fluctuations of the local fields; these fluctuations are especially large in composites with fractal morphology.[5,15,16] Nanostructured composite materials are potentially of great practical importance as media with an intensity-dependent dielectric function and, in particular, as nonlinear filters and optical bistable elements. A typical system under consideration is a composite material in which a nonlinear material is embedded in a host medium which can be linear or nonlinear. The response of a nonlinear composite can be tuned by controlling the volume fraction and morphology of constitutes.

Stroud and Hui,[1] and Flytzanis with co-workers,[7] considered the electromagnetic response of nonlinear particles randomly embedded in a linear host in the dilute limit when the interaction between particles is small. Perturbation expansions that allow one to determine small corrective terms for nonlinear susceptibility were developed by Yu, Hui, Stroud, and their co-workers[8] (some related problems, including the case of spherical nonlinear inclusions, have also been studied by Bergman with co-workers[6]). These authors also considered the case where inclusions and host material may possess nonlinearities up to the fifth order.

Sipe and Boyd studied nonlinear susceptibility of composites within the Maxwell-Garnett model.[9] Hui and Stroud have generalized the differential effective-medium approximation, which they developed previously to model the effective linear response of a fractal cluster, to treat the effective nonlinear response.[10] Their analysis showed that the clustering of particles can result in an appreciable enhancement of the nonlinear response per particle (relative to the totally random case) only when a host is a better conductor than the nonlinear inclusion. A similar conclusion was obtained by Yu who applied a multifractal analysis of the voltage distribution for a deterministic fractal cluster embedded in the hierarchical lattice.[11]

Strong enhancement of nonlinear susceptibilities at zero frequency near a percolation threshold was pointed out by Zhang and Stroud.[12] Critical behavior of nonlinear composites near the percolation threshold was also analyzed by Hui and by Yu with co-workers.[13] Using the effective-medium approximation (EMA) and the transfer-matrix numerical simulations for random networks, Zhang and Stroud have obtained a strong enhancement of cubic nonlinear susceptibility in a metal-insulator composite near surface-plasmon resonances.[12] Recently, Levy, Bergman, and Stroud showed that an induced cubic nonlinearity can be generated in a composite, even though none of its components possess it intrinsically.[14]

The aggregation of particles often results in fractal clusters. The number of monomers in a fractal cluster, N, scales as $N=(R_c/R_0)^D$, where D is an index called the Hausdorff dimension, R_c is the radius of gyration, and R_0 is a typical separation between nearest neighbors. The pair-correlation function, $g(r)$, in a fractal cluster also has a power-law dependence, $g(r) \propto r^{D-d}$, where d is the dimension of the embedding space. A fractal is called nontrivial if $D<3$.

Shalaev and his co-workers[2–5] studied nonlinear optical properties of fractal aggregates and showed that the aggregation of initially isolated particles into fractal clusters results in a huge enhancement of the nonlinear response within the spectral range of collective dipolar resonances (e.g., surface-plasmon resonances). The eigenmodes were found by diagonalizing the interaction operator of the dipoles induced by light on particles forming the cluster. Giant fluctuations of the local fields were studied by Stockman with co-workers.[16] Many of the dipolar eigenmodes are strongly localized in different parts of a cluster with random local structure[16–18] (however, there are delocalized modes as well); this leads ultimately to strong fluctuations of local fields in fractals.

The prediction of a huge enhancement of optical nonlinearities in fractal clusters[2] was then confirmed

experimentally[3] for the example of degenerate four-wave mixing (DFWM). Aggregation of initially isolated silver particles into fractal clusters in this experiment led to a 10^6-fold enhancement of the efficiency of the nonlinear four-wave process.

Numerical simulations of the nonlinear optical response in fractal clusters have been previously performed for the special case of diluted clusters.[19] This model can describe, in particular, nanoparticles in a fractal host such as a polymer-tree. In the central part of the diluted cluster spectrum, the nonlinear optical response scales as a function of the generalized frequency variable,[4] whereas, in the wing, the response can be well described by the binary approximation.[2]

In this paper we present large-scale numerical simulations for a number of nonlinear optical processes in composite materials consisting of original nondiluted fractal clusters. In particular, the model of cluster-cluster aggregates (CCA's) with $D \approx 1.78$, that provides a good description of metal colloid aggregates, is used in the simulations. The results of calculations are averaged over an ensemble of 500-particle CCA's. Particles in a cluster are assumed to interact via light-induced dipolar fields resulting in the formation of collective eigenmodes. The simulations are based on exact formulas, describing the nonlinear optical responses in an arbitrary (fractal or nonfractal) small-particle composite. These formulas are expressed in terms of the ensemble-average products of local fields (or local linear polarizabilities) that are found through the decomposition over the dipolar eigenmodes of a cluster. A comparison with available experimental data is also performed.

The paper is organized as follows. In Sec. II we present the results of calculations of local-field intensities in fractal and nonfractal clusters. In Sec. III we derive formulas that describe enhanced optical processes in composites and present the results of our numerical simulations. Specifically, we consider the following optical phenomena: four-wave mixing, harmonic generation, Raman scattering, and nonlinear refraction and absorption in Kerr media. The obtained results are briefly summarized and discussed in concluding Sec. IV.

II. ENHANCED LOCAL FIELDS IN SMALL-PARTICLE COMPOSITES

Similar to the preceding paper,[20] we consider a system of N polarizable particles (monomers) with the dipole-dipole interactions between them at the optical frequency. The monomers are positioned at the points $\mathbf{r}_i$ $(i=1,\ldots,N)$ and assumed to be much smaller than the wavelength, λ, of the incident wave. For the sake of simplicity we restrict our consideration to the quasistatic limit (i.e., assume that $R_c \ll \lambda$). Then, the interaction operator has the form

$$W^{ij}_{\alpha\beta} \equiv (i\alpha|W|j\beta) = \begin{cases} [\delta_{\alpha\beta} - 3n^{(ij)}_{\alpha} n^{(ij)}_{\beta}] r^{-3}_{ij}, & i \neq j, \\ 0, & i = j, \end{cases} \tag{1}$$

where Greek indices stand for Cartesian components (the summation over repeated Greek indices is implied), $\mathbf{r}_{ij} \equiv \mathbf{r}_i - \mathbf{r}_j$, and $\mathbf{n}^{(ij)} \equiv \mathbf{r}_{ij}/r_{ij}$.

The enhancement of optical processes in a small-particle composite occurs because local fields exhibit strong fluctuations that significantly exceed the applied field. The local field, $\mathbf{E}_i$, acting on the ith particle (monomer) in a cluster can be found from the theory of the linear optical response:[20]

$$E_{i\alpha} = \alpha_0^{-1} \alpha_{i,\alpha\beta} E^{(0)}_{\beta}, \tag{2}$$

where $\mathbf{E}^{(0)}$ is the applied field, α_0 is the polarizability of the individual monomer, and $\alpha_{i,\alpha\beta}$ is the local polarizability of a monomer in a cluster which is related to the local dipole moment $d_{i\alpha}$ induced on the ith particle via the formula $d_{i\alpha} = \alpha_{i,\alpha\beta} E^{(0)}_{\beta}$ [cf., Eq. (13) of the preceding paper[20]]. Note that since we restrict our consideration to the quasistatic approximation, by $\mathbf{E}^{(0)}$, $\mathbf{E}_i$, and $\mathbf{d}_i$ we mean the amplitudes of the fields and dipoles, i.e., the spatial- and time-varying factors are omitted. By solving the coupled-dipole equations (CDE's) in the quasistatic approximation, we obtain [see Eqs. (1), (7), and (12) of the preceding paper[20]]

$$\alpha_{i,\alpha\beta} = \sum_{nj} \frac{(i\alpha|n)(n|j\beta)}{(w_n - X) - i\delta}, \tag{3}$$

where $X \equiv -\mathrm{Re}[\alpha_0^{-1}]$, $\delta \equiv -\mathrm{Im}[\alpha_0^{-1}]$, and w_n and $|n)$ are the eigennumbers and eigenvectors of the interaction operator: $(n|W|m) = w_n \delta_{nm}$; accordingly, $(i\alpha|n)$ are the components of the vector $|n)$ in the orthogonal basis $|i\alpha)$ (see the preceding paper[20]).

The light frequency ω enters in the basic equations (2) and (3) implicitly via the complex variable $Z = \alpha_0^{-1}(\omega) \equiv -[X + i\delta]$. Material and geometrical properties of monomers affect the problem only via the parameter Z. The real part, $X = X(\omega)$, plays the role of a spectral variable instead of ω, and the imaginary part, $\delta > 0$, describes dissipation in a monomer; in general, δ can also depend on ω. (Note that α_0 may describe not only the polarizability of a simple monomer, such as a sphere, but also the polarizability of a composite monomer, such as a coated sphere.) The dependences of X and δ on ω for some real systems are discussed in the preceding paper.[20]

The parameter characterizing enhancements of the local-filed intensities can be defined as follows:

$$G = \langle |E_i|^2 \rangle / |E^{(0)}|^2, \tag{4}$$

where the symbol $\langle \cdots \rangle$ denotes an average over an ensemble of random clusters. As shown in Ref. 16, the enhancement G is related to the cluster absorption, $\mathrm{Im}\,\alpha(X) = (1/3)\mathrm{Im}\langle \alpha_{i,\alpha\alpha} \rangle$, as follows:

$$G = \delta[1 + X^2/\delta^2]\mathrm{Im}\alpha(X). \tag{5}$$

According to (5), the enhancement factor $G \approx (X^2/\delta)\mathrm{Im}\alpha$ for $|X| \gg \delta$, i.e., it can be very large, if $\mathrm{Im}\alpha(X)$ is not too small. Thus, we anticipate a huge enhancement for a system with a strong inhomogeneous broadening, when $\mathrm{Im}\alpha(X)$ is relatively large in a wide range of $|X|$, including $|X| \gg \delta$. (Clearly, in the far Lorentz wing, when $|X| \to \infty$, the absorption is $\mathrm{Im}\alpha \approx \delta/X^2$ and $G \approx 1$.)

As shown in the preceding paper (cf., Figs. 1, 2, and 3 of Ref. 20), inhomogeneous broadening in fractal cluster-cluster aggregates (CCA's) is significantly larger than in nonfractal composites, such as a random gas of particles (RGP) and a close-packed sphere of particles (CPSP). (For details on the mentioned models and on the corresponding numerical simu-

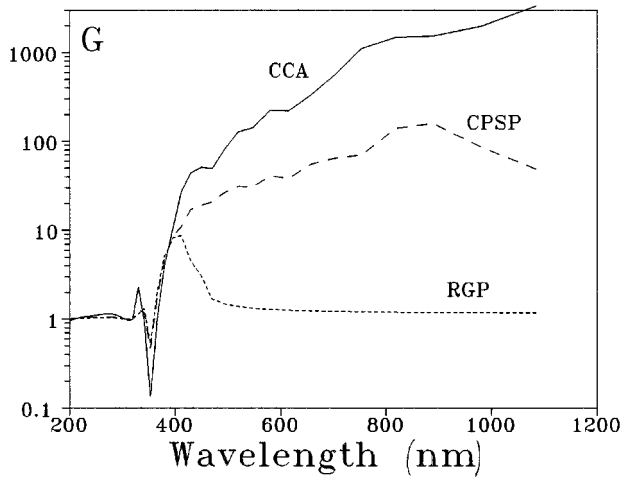

FIG. 1. Enhancement factors, G, of local field intensities plotted against λ for 500-particle aggregates: fractal cluster-cluster aggregates, CCA's (solid line), a random gas of particles (RGP) with the same as for CCA's volume fraction of metal (short-dashed line), and a close-packed sphere of particles, CPSP (long-dashed line).

lations, see Sec. III of Ref. 20.) Accordingly, we expect a significantly larger enhancement of the local field-intensities in fractal CCA's.

Note that, since in fractals the fluctuations are very large so that $\langle|E|^2\rangle \gg \langle|E|\rangle^2$,[5,16] we have $\langle|\Delta E|^2\rangle \approx \langle|E|^2\rangle$; therefore, in this case, G characterizes both the enhancement of local fields and their fluctuations as well. In other words, the larger fluctuations, the stronger enhancement.

Below we present the results of calculations of G for various small-particle composites. All quantities are expressed in units such that the diameter of a particle, a, is equal to one. Our simulations were performed for 500-particle clusters and were averaged over an ensemble of 10 random cluster realizations.[21–25]

In Fig. 1 we show the results of simulations for the enhancement factor, G, in silver CCA's in vacuum compared with that for nonfractal composites, RGP and CPSP. [In contrast to calculations of the preceding paper,[20] the material constants of silver were taken here from Ref. 26 instead of Ref. 27; these two sources give slightly different values of $\epsilon(\lambda)$. Further, no possible corrections associated with electron scattering are taken into account.] For the quantities $X(\lambda)$ and $\delta(\lambda)$ in (5), we used formulas (21)–(23) of the preceding paper[20] (the factor $2k^3/3$ in the expression for δ was neglected). The quantity $\alpha(X)$ was calculated by numerically solving the CDE's in the quasistatic limit; in this limit, the interaction operator, $\hat{G} \equiv -\hat{V}$, in Eq. (1) of the preceding paper[20] is equal to the $\hat{W}$ defined above. To solve the CDE's, we used the method based on the diagonalization of the interaction matrix W (for details, see Sec. III of the preceding paper.[20])

As seen in Fig. 1, the enhancement of local-field intensities in fractal CCA's is significantly larger than in nonfractal RGP and CPSP clusters, as was anticipated. The enhancement can reach very high values, $\sim 10^3$, and increases with λ. This occurs because both the localization of fractal eigenmodes and their mode quality factor ($q \sim 1/\delta \sim |\epsilon - \epsilon_h|^2/3\epsilon''\epsilon_h$) increase for the modes located in the long-wavelength part of the spectrum [see also Fig. 5 and Eq. (21) of the preceding paper[20]].

We next consider a more detailed comparison between fractal small-particle composites and non-fractal inhomogeneous media (see also the discussion in Sec. VI of Ref. 20). The simulations were performed for RGP and CCA's having the same volume fraction, p, filled by metal. The value of p in a fractal cluster is very small (in fact, $p \to 0$ at $R_c \to \infty$). According to the Maxwell-Garnett theory,[6] there is only one resonant frequency in conventional ($d=D$) media with $p \ll 1$; the resonance is just slightly shifted from the resonance of an isolated particle occurring at $X(\omega)=0$. In contrast, in fractal media, despite the fact that p is asymptotically zero, there is a high probability, $\propto r^{D-d}$, of finding a number of particles in close proximity to any chosen one. Thus, in fractals, there is always a strong interaction of a particle with others distributed in its random neighborhood. As a result, there exist localized eigenmodes with distinct spatial orientations in different parts of a cluster, where the location depends on the frequency and polarization characteristics of the mode. As mentioned above, some of these modes are significantly shifted to the long-wavelength part of the spectrum where their quality factors, q, are much larger than that for a noninteracting particles at $X(\omega)=0$. Thus, the dipole-dipole interaction of constituent particles in a fractal cluster "generates" a wide spectral range of resonant modes with enhanced quality factors and with spatial locations which are very sensitive to the frequency and polarization of the applied field. The localization of modes in various random parts of a cluster also brings about giant spatial fluctuations of the local fields, when one moves from "hot" to "cold" zones corresponding to high and low field-intensity areas, respectively.

In the case of a CPSP, the volume fraction, p, is not small. However, since the dipole-dipole interaction for a three-dimensional CPSP is long range, one expects that eigenmodes are delocalized over the whole sample, so that all particles are involved in the excitation. Accordingly, fluctuations (and enhancements) of local fields are much smaller than in a fractal aggregate where the modes are localized.

As seen in Fig. 1, enhancements and fluctuations of local fields in CPSP and RGP are significantly less than those in the case of fractal CCA's, in accordance with the above arguments.

The enhanced local fields result in enhancements of optical processes considered below. Based on the simulations presented above, we anticipate that in fractal composites, where the fluctuations are especially strong, the enhancements can be very large. Below, we analyze various enhanced optical phenomena in a composite material consisting of fractal CCA's.

III. ENHANCED OPTICAL PROCESSES

In this section we consider the intensity-dependent dielectric function associated, in particular, with the Kerr optical nonlinearity and harmonic generation. Enhanced Raman scattering is also analyzed. (Note that although spontaneous Raman scattering is a linear optical process, its enhancement, as will be shown, is $\sim \langle|E_i/E^{(0)}|^4\rangle$, i.e., has a nonlinear de-

pendence on the field and, therefore, we consider the enhanced Raman scattering in this paper which is concerned with nonlinear optics.) We derive formulas for enhancement factors for various optical processes in a small-particle composite and perform numerical simulations based on these formulas.

A. Four-wave mixing

Four-wave mixing (FWM) is determined by the nonlinear polarizability[28]

$$\beta^{(3)}_{\alpha\beta\gamma\delta}(-\omega_s;\omega_1,\omega_1,-\omega_2), \tag{6}$$

where $\omega_s=2\omega_1-\omega_2$ is the generated frequency, and ω_1 and ω_2 are the frequencies of the applied waves. Coherent anti-Stokes Raman scattering (CARS) is an example of FWM. In one elementary CARS process, two ω_1 photons are transformed into ω_2 and ω_s photons. Another example is degenerate FWM (DFWM); this process is used in optical phase conjugation (OPC) which results in complete removal of optical aberrations.[28] In DFWM, all waves have the same frequency ($\omega_s=\omega_1=\omega_2$) and differ only by their propagation directions and, in general, by polarizations. In a typical OPC experiment, two oppositely directed pump beams, with field amplitudes $\mathbf{E}^{(1)}$ and $\mathbf{E}'^{(1)}$, and a probe beam, with amplitude $\mathbf{E}^{(2)}$ (and propagating at a small angle to the pump beams), result in an OPC beam which propagates against the probe beam. Because of the interaction geometry, the wave vectors of the waves satisfy to the relation $\mathbf{k}_1+\mathbf{k}_1'=\mathbf{k}_2+\mathbf{k}_s=0$. Clearly, for the two pairs of oppositely directed beams, that have the same frequency ω, the phase-matching conditions are automatically fulfilled.[28]

Below we consider DFWM process where the total applied field is $\mathbf{E}^{(0)}=\mathbf{E}^{(1)}+\mathbf{E}'^{(1)}+\mathbf{E}^{(2)}$. The nonlinear polarizability, $\beta^{(3)}$, that results in DFWM, also leads to nonlinear refraction and absorption (to be considered in Sec. III D) and is associated with the Kerr optical nonlinearity. For coherent effects, including the ones discussed in this section, averaging is performed over a generated field amplitude (rather than intensity) or, equally, over nonlinear polarizability. Note also that the nonlinear polarizability, $\beta^{(3)}$, can be associated with either monomers or molecules adsorbed on them.

The orientation-average nonlinear polarizability in an isotropic medium can be expressed, in general, through two independent scalar functions f_s and f_a as[28]

$$\langle\beta^{(3)}_{\alpha\beta\gamma\delta}\rangle_0=f_s\Delta^{+}_{\alpha\beta\gamma\delta}+f_a\Delta^{-}_{\alpha\beta\gamma\delta}, \tag{7}$$

$$\Delta^{+}_{\alpha\beta\gamma\delta}=\frac{1}{3}\{\delta_{\alpha\beta}\delta_{\gamma\delta}+\delta_{\alpha\gamma}\delta_{\beta\delta}+\delta_{\alpha\delta}\delta_{\beta\gamma}\}, \tag{8}$$

$$\Delta^{-}_{\alpha\beta\gamma\delta}=\frac{1}{3}\{\delta_{\alpha\beta}\delta_{\gamma\delta}+\delta_{\alpha\gamma}\delta_{\beta\delta}-2\,\delta_{\alpha\delta}\delta_{\beta\gamma}\}, \tag{9}$$

where the symbol $\langle\cdots\rangle_0$ denotes an average over orientations. The terms $f_s\Delta^{+}$ and $f_a\Delta^{-}$ are totally and partially symmetric parts of $\beta^{(3)}$, respectively (over $\alpha\beta$ and $\gamma\delta$).

When a cluster consists of monomers, the field acting upon them is the local field $\mathbf{E}_i$ rather than the applied field $\mathbf{E}^{(0)}$. Also, the dipolar interaction of nonlinear dipoles should be included. Taking these arguments into account, we write the following system of equations for the light-induced nonlinear dipoles:

$$d^{\mathrm{NL}}_{i,\alpha}=3\beta^{(3)}_{\alpha\beta\gamma\delta}E_{i,\beta}E_{i,\gamma}E^{*}_{i,\delta}+\alpha(\omega_s)\sum_j W^{ij}_{\alpha\beta}d^{\mathrm{NL}}_{j,\beta}, \tag{10}$$

where the prefactor 3 represents the degeneracy factor that gives the number of distinct permutations of the frequencies ω, ω, and $-\omega$.[28]

Hereafter, we assume that the corrections to the local field E_i associated with nonlinear dipole moments d_i^{NL} are small and can be neglected. This allows us to find E_i [see Eqs. (2) and (3)] by solving first the CDE's for linear dipoles d_i, and, then, to substitute these fields to the CDE's (10) for nonlinear dipoles d_i^{NL}.

Using similar procedures that were used to solve the CDE's for linear dipoles [see Eqs. (5)–(7) of the preceding paper[20] and Eqs. (2) and (3) of this paper], we obtain the solution of (10) in the form

$$d^{\mathrm{NL}}_{i\alpha}=3Z\beta^{(3)}_{\beta'\beta\gamma\delta}\sum_{nj}\Lambda_n(i\alpha|n)(n|j\beta')E_{j,\beta}E_{j,\gamma}E^{*}_{j,\delta}. \tag{11}$$

Substituting the expression (2) for the local fields $\mathbf{E}_i$, we find for the mean nonlinear dipole moment

$$\langle d^{\mathrm{NL}}_{i\alpha}\rangle=3\langle\beta^{(3c)}_{\alpha\beta\gamma\delta}\rangle E^{(0)}_{\beta}E^{(0)}_{\gamma}E^{(0)*}_{\delta}, \tag{12}$$

where

$$\langle\beta^{(3c)}_{\alpha\beta\gamma\delta}\rangle=Z^3Z^{*}\langle\beta^{(3)}_{\alpha'\beta'\gamma'\delta'}\rangle_0\langle\alpha_{j,\alpha'\alpha}\alpha_{j,\beta'\beta}\alpha_{j,\gamma'\gamma}\alpha^{*}_{j,\delta'\delta}\rangle \tag{13}$$

represents the effective nonlinear polarizability of a particle in a cluster. To obtain (13), we assumed that averaging over the orientations of a nonlinear particle and averaging over an ensemble of clusters can be performed independently.

The substitution of $\langle\beta^{(3)}_{\alpha\beta\gamma\delta}\rangle_0$ from (7)–(9) into (13) results in several products like the following

$$\delta_{\alpha'\beta'}\delta_{\gamma'\delta'}[\alpha_{j,\alpha'\alpha}\alpha_{j,\beta'\beta}\alpha_{j,\gamma'\gamma}\alpha^{*}_{j,\delta'\delta}]=(\hat{\alpha}_j^T\hat{\alpha}_j)_{\alpha\beta}(\hat{\alpha}_j^T\hat{\alpha}_j^{*})_{\gamma\delta} \tag{14}$$

where $(\hat{\alpha}_j^T\hat{\alpha}_j)_{\alpha\beta}\equiv\alpha_{j,\alpha'\alpha}\alpha_{j,\alpha'\beta}$, and $(\hat{\alpha}_J^T\hat{\alpha}_j^{*})_{\gamma\delta}\equiv\alpha_{j,\beta'\gamma}\alpha^{*}_{j,\beta'\delta}$ (the T symbol in $\hat{\alpha}^T$ denotes a transposition of the matrix $\hat{\alpha}$). Averaging over the orientations in (14) gives

$$\begin{aligned}\langle(\hat{\alpha}_j^T\hat{\alpha}_j)_{\alpha\beta}(\hat{\alpha}_j^T\hat{\alpha}_j^{*})_{\gamma\delta}\rangle_0&=\frac{1}{15}\delta_{\alpha\beta}\delta_{\gamma\delta}[2\,\mathrm{Tr}(\hat{\alpha}_j^T\hat{\alpha}_j)\mathrm{Tr}(\hat{\alpha}_j^T\hat{\alpha}_j^{*})\\&-\mathrm{Tr}(\hat{\alpha}_j^T\hat{\alpha}_j\hat{\alpha}_j^T\hat{\alpha}_j^{*})]+\frac{1}{30}(\delta_{\alpha\gamma}\delta_{\beta\delta}+\delta_{\alpha\delta}\delta_{\beta\gamma})\\&\times[3\,\mathrm{Tr}(\hat{\alpha}_j^T\hat{\alpha}_j)\mathrm{Tr}(\hat{\alpha}_j^T\hat{\alpha}_j^{*})-\mathrm{Tr}(\hat{\alpha}_j^T\hat{\alpha}_j\hat{\alpha}_j^T\hat{\alpha}_j^{*})].\end{aligned} \tag{15}$$

[Formula (15) can be proved by performing a contraction over all pairs of indices.]

Proceeding similarly with the other products of the δ symbols [originating from $\Delta^{\pm}_{\alpha\beta\gamma\delta}$ in (7)–(9)] and polarizabilities α_i in (13), we obtain

$$\langle \beta^{(3c)}_{\alpha\beta\gamma\delta} \rangle = F_s \Delta^{+}_{\alpha\beta\gamma\delta} + F_a \Delta^{-}_{\alpha\beta\gamma\delta}, \tag{16}$$

where

$$F_s = \frac{1}{15} Z^3 Z^* f_s \langle \mathrm{Tr}(\hat{\alpha}_i^T \hat{\alpha}_i)\mathrm{Tr}(\hat{\alpha}_i^T \hat{\alpha}_i^*) + 2\ \mathrm{Tr}(\hat{\alpha}_i^T \hat{\alpha}_i \hat{\alpha}_i^T \hat{\alpha}_i^*) \rangle, \tag{17}$$

$$F_a = \frac{1}{6} Z^3 Z^* f_a \langle \mathrm{Tr}(\hat{\alpha}_i^T \hat{\alpha}_i)\mathrm{Tr}(\hat{\alpha}_i^T \hat{\alpha}_i^*) - \mathrm{Tr}(\hat{\alpha}_i^T \hat{\alpha}_i \hat{\alpha}_i^T \hat{\alpha}_i^*) \rangle. \tag{18}$$

According to (16), the symmetry of the nonlinear polarizability of an isolated monomer [see (7)–(9)], is reproduced in the mean polarizability of a cluster. The totally symmetric part of the monomer's nonlinear polarizability ''generates'' a totally symmetric part of the cluster polarizability ($F_s \propto f_s$); the same is valid for the partially symmetrical parts ($F_a \propto f_a$).

If the laser frequency lies far outside a band of the resonant modes of a cluster, i.e., $|X(\omega)|$ is much larger than all $|w_n|$ in (3), then, $\alpha_i \approx \alpha_0$ for all i (recall that $Z = \alpha_0^{-1}$). In this case, the interaction between particles in a cluster is not important, and, as follows from (17) and (18), $F_s = f_s$ and $F_a = f_a$, i.e., the nonlinear polarizability of a particle in a composite is equal to that of an isolated particle.

We now consider the enhancement of DFWM that accompanies the aggregation of particles into clusters. Let particles be first randomly embedded and well separated in a linear host medium. We assume that the volume fraction, p, that the particles occupy is small and one can neglect their interaction. Then, let particles aggregate in many random clusters that are relatively far from each other (i.e., the inter-cluster interaction is still negligible). Thus, after the aggregation, we obtain a mixture of many clusters (each cluster may consist of thousands of particles). The average volume fraction filled by particles remains, obviously, the same. However, particles within one cluster now strongly interact via light-induced dipolar fields.

The described scenario of aggregation occurs, for example, in a silver colloid solution. In that case one first produces a silver sol (nonaggregated particles in solution), e.g., by reducing silver nitrate with sodium borohydride.[24] Addition of an adsorbent (like phthalizine) promotes aggregation, forming fractal colloid clusters with fractal dimension $D \approx 1.78$ (see also the preceding paper[20]).

Before the aggregation, the nonlinear polarization, $\mathbf{P}^{(3)}$, of particles in a spherically isotropic medium can be presented as[28]

$$\mathbf{P}^{(3)}(\omega) = a\mathbf{E}^{(0)}(\mathbf{E}^{(0)} \cdot \mathbf{E}^{(0)*}) + \frac{1}{2} b \mathbf{E}^{(0)*}(\mathbf{E}^{(0)} \cdot \mathbf{E}^{(0)}), \tag{19}$$

where the coefficients a and b are related to f_s and f_a introduced in (7) as follows:

$$a = \frac{2}{3}(f_s + f_a) p v_0^{-1}, \quad b = \frac{2}{3}(f_s - 2f_a) p v_0^{-1} \tag{20}$$

with v_0 being the volume of one particle [for a sphere, $v_0 = (4\pi/3)R_m^3$].

Since after the aggregation the medium remains isotropic, on average, the nonlinear polarization, $P^{(3c)}$, of a composite consisting of clusterized particles has similar to (19) form

$$\mathbf{P}^{(3c)}(\omega) = A\mathbf{E}^{(0)}(\mathbf{E}^{(0)} \cdot \mathbf{E}^{(0)*}) + \frac{1}{2} B \mathbf{E}^{(0)*}(\mathbf{E}^{(0)} \cdot \mathbf{E}^{(0)}), \tag{21}$$

where A and B, are given by

$$A = \frac{2}{3}(F_s + F_a) p v_0^{-1}, \quad B = \frac{2}{3}(F_s - 2F_a) p v_0^{-1}, \tag{22}$$

with F_s and F_a defined in (17) and (18), respectively. Note that expression (21) contains terms $\propto (\mathbf{E}^{(1)} \cdot \mathbf{E}'^{(1)})\mathbf{E}^{(2)*}$ that lead to a OPC signal in DWFM; it also contains the terms leading to the Kerr nonlinear refraction (see Sec. III D).

The nonlinear susceptibility, $\bar{\chi}^{(3c)}_{\alpha\beta\gamma\delta}$, of a composite material is defined via the relation

$$P^{(3c)}_{\alpha}(\omega) = 3\bar{\chi}^{(3c)}_{\alpha\beta\gamma\delta}(-\omega;\omega,\omega,-\omega) E^{(0)}_{\beta} E^{(0)}_{\gamma} E^{(0)*}_{\delta},$$

where $\bar{\chi}^{(3c)}_{\alpha\beta\gamma\delta}$ can be expressed in terms of the ensemble-average nonlinear polarizability, $\langle \beta^{(3c)}_{\alpha\beta\gamma\delta} \rangle$, as follows:

$$\bar{\chi}^{(3c)}_{\alpha\beta\gamma\delta}(-\omega;\omega,\omega,-\omega) = p v_0^{-1} \langle \beta^{(3c)}_{\alpha\beta\gamma\delta}(-\omega;\omega,\omega,-\omega) \rangle. \tag{23}$$

In particular, if $\beta^{(3)}$ is due to nonresonant electronic response of adsorbate molecules (the aggregate modes, however, can be in resonance with the exciting field), the following relation is valid: $a = b$,[28] i.e., $f_a = 0$ [see Eqs. (20)], and, using (17), (18), (20), and (22), we obtain

$$\frac{A}{a} = \frac{B}{b} = \frac{F_s}{f_s}. \tag{24}$$

The efficiency of four-wave mixing is proportional to the generated amplitude squared, and the enhancement due to particle clustering is given by

$$\begin{aligned} G_{\mathrm{FWM}} &= |F_s / f_s|^2 \\ &= \frac{(X^2 + \delta^2)^4}{225} \\ &\quad \times |\langle \mathrm{Tr}(\hat{\alpha}_i^T \hat{\alpha}_i)\mathrm{Tr}(\hat{\alpha}_i^T \hat{\alpha}_i^*) + 2\ \mathrm{Tr}(\hat{\alpha}_i^T \hat{\alpha}_i \hat{\alpha}_i^T \hat{\alpha}_i^*) \rangle|^2. \end{aligned} \tag{25}$$

We can easily generalize (25) for the case of a nondegenerate FWM, such as CARS:

$$\begin{aligned} G_{\mathrm{FWM}} &= |F_s / f_s|^2 \\ &= \frac{(X^2 + \delta^2)^4}{225} \\ &\quad \times |\langle \mathrm{Tr}[\hat{\alpha}_i^T(\omega_s)\hat{\alpha}_i(\omega_1)]\mathrm{Tr}[\hat{\alpha}_i^T(\omega_1)\hat{\alpha}_i^*(\omega_2)] \\ &\quad + 2\ \mathrm{Tr}[\hat{\alpha}_i(\omega_s)^T \hat{\alpha}_i(\omega_1)\hat{\alpha}_i^T(\omega_1)\hat{\alpha}_i^*(\omega_2)] \rangle|^2. \end{aligned}$$

For a nonresonant excitation, when $|X(\omega)| \gg |w_n|$ and therefore $\alpha_i \approx \alpha_0$, we see from (25) that $G = 1$, i.e., there is no enhancement in this case.

We consider now the expression (25) in more detail and introduce the quantity g_{FWM} defined as

$$g_{\mathrm{FWM}} \equiv \mathrm{Tr}(\hat{\alpha}_i^T \hat{\alpha}_i)\mathrm{Tr}(\hat{\alpha}_i^T \hat{\alpha}_i^*) + 2\ \mathrm{Tr}(\hat{\alpha}_i^T \hat{\alpha}_i \hat{\alpha}_i^T \hat{\alpha}_i^*). \tag{26}$$

Using (3), this expression can be transformed to

$$g_{\mathrm{FWM}}=\sum_{nmlk}[M_{nmlk}+2K_{nmlk}]\Lambda_n\Lambda_m\Lambda_l\Lambda_k^*, \tag{27}$$

where $\Lambda_n\equiv[(w_n-X)-i\delta]^{-1}$,

$$M_{nmlk}\equiv\sum_{jj'j''j'''}(i\alpha|n)(n|j\beta)(i\alpha|m)(m|j'\beta)\times(i\alpha'|l)(l|j''\beta')(i\alpha'|k)(k|j'''\beta'), \tag{28}$$

and

$$K_{nmlk}\equiv\sum_{jj'j''j'''}(i\alpha|n)(n|j\beta)(i\alpha|m)(m|j'\beta')\times(i\beta''|l)(l|j''\beta')(i\beta''|k)(k|j'''\beta). \tag{29}$$

According to (25) and (26), the enhancement factor, G_{FWM}, has the form

$$G_{\mathrm{FWM}}=\frac{(X^2+\delta^2)^4}{225}|\langle g_{\mathrm{FWM}}(X)\rangle|^2. \tag{30}$$

Performing the integration in (27), we find the following sum rule for function g_{FWM}:

$$\int_{-\infty}^{\infty}g_{\mathrm{FWM}}(X)dX=2\pi i\sum_{nmlk}[M_{nmlk}+2K_{nmlk}]R_{nk}R_{mk}R_{lk}, \tag{31}$$

where

$$R_{nm}\equiv\frac{1}{2i\delta+(w_n-w_m)}. \tag{32}$$

The product of the Λ factors in Eq. (27) can be rewritten as

$$\Lambda_n\Lambda_m\Lambda_l\Lambda_k^*=R_{lk}\{\Lambda_n\Lambda_m\Lambda_l-R_{mk}\Lambda_n\Lambda_m+R_{nk}R_{mk}(\Lambda_n-\Lambda_k^*)\}. \tag{33}$$

It is instructive to find first g^r_{FWM} which is due to the ''resonant'' difference of the eigenmodes in (27), i.e., to calculate the contribution of only those modes for which $|w_n-w_m|\ll\delta$. In this case, the R factors become very large. Then, retaining in (33) only the term with the highest power of R and using (3), we obtain from (27)–(29) the following ensemble-average expression:

$$\langle g^r_{\mathrm{FWM}}(X)\rangle=-\frac{15}{4\delta^3}\,\mathrm{Im}\alpha(X). \tag{34}$$

The quantity $\langle g^r_{\mathrm{FWM}}(X)\rangle$ satisfies the sum rule

$$\int_{-\infty}^{\infty}\langle g^r_{\mathrm{FWM}}(X)\rangle dX=-\frac{15\pi}{4\delta^3}. \tag{35}$$

For diluted clusters, it was shown that the enhancement factor is closely approximated by the resonant contribution.[4] Our conjecture is that for the case of nondiluted clusters the expression $\langle g^r_{\mathrm{FWM}}(X)\rangle$ also describes properly the functional dependence on X and δ. Then, the enhancement factor, G_{FWM}, can be presented as

$$G_{\mathrm{FWM}}\approx C_{\mathrm{FWM}}\frac{(X^2+\delta^2)^4}{\delta^6}[\mathrm{Im}\alpha(X)]^2, \tag{36}$$

where the prefactor, C_{FWM}, should be considered as an adjustable parameter.

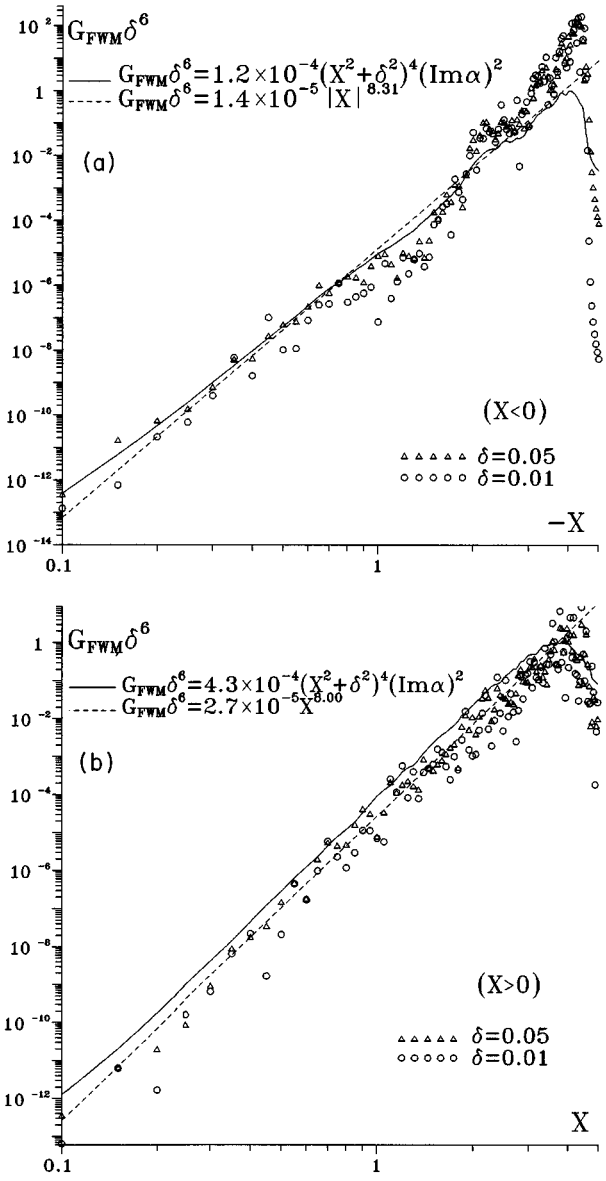

FIG. 2. The enhancement of degenerate or nearly degenerate four-wave mixing, G_{FWM}, in CCA's for negative (a) and positive (b) values of the spectral variable, X. See the text for further explanations.

In Fig. 2, we show the results of numerical calculations of the enhancement factor, G_{FWM}, in CCA's for $X<0$ (a) and $X>0$ (b). The simulations were performed using formulas (25) and (3). The solid lines in Fig. 2 describe the results of calculations based on formula (36), with C_{FWM} found from the relation $G_{\mathrm{FWM}}\delta^6=1$ in its maxima, occurring at $X\approx\pm4$. The dashed lines represent a power-law fit for the

range $0.1 \leqslant |X| \leqslant 3$ ($\delta = 0.05$). The computed exponents (8.31 ± 1.00 for $X<0$ and 8.00 ± 1.00 for $X>0$) are close to 8 for both positive and negative values of X. This value for the exponent is not surprising, since, within the interval $|X| \leqslant 3$, the dependence of $\mathrm{Im}\alpha$ on X (see Fig. 1 of the preceding paper[20]) in (36) is relatively weak in comparison with that which is due to the factor X^8 in (25) and (36). This X dependence differs from that obtained for diluted CCA's, where the absorption has a scaling dependence, $\mathrm{Im}\,\alpha \sim |X|^{d_o - 1}$, with $d_o \approx 0.3 \pm 0.1$,[21] and $G_{\mathrm{FWM}} \propto |X|^{6+2d_o}$, in accordance with (36).[4]

As seen in Fig. 2, the enhancement strongly increases toward larger values of $|X|$. This occurs because the local fields become stronger for larger values of $|X|$ (according to Fig. 1, the local-field intensities increase in the long-wavelength part of the spectrum which corresponds to larger $|X|$ with $X<0$).

It also follows from Fig. 2 that the product $G_{\mathrm{FWM}}\delta^6$ remains, on average, the same for the two very different values of δ, 0.01 and 0.05. This indicates that, in accordance with (36), the enhancement is proportional to the sixth power of the resonance quality factor, $G_{\mathrm{FWM}} \propto q^6$ ($q \sim \delta^{-1}$) and reaches huge values in the maxima occurring at $X \approx \pm 4$.

In the end of this section, we mention that a millionfold enhancement of DFWM due to the clustering of initially isolated silver particles in a colloidal solution was experimentally obtained in Ref. 3. For spherical particles of radius R_m, the value of X and δ can be obtained from formulas (21) and (22) of the preceding paper.[20] Using the data of Ref. 26 for the material constants in silver, we find that for $\lambda = 532$ nm (used in the experiment) $X \approx -2.55$ and $\delta \approx 0.05$. The coefficient R_m^{-3} in Eqs. (21) and (22) of Ref. 20, measured in units of $a=1$, was chosen to be as $R_m^{-3} \equiv (a/R_m)^3 = 4\pi/3$ (for details, see Sec. V of the preceding paper[20]).

As seen in Fig. 2(a), for $X=-2.55$ and $\delta=0.05$, the value of G_{FWM} is $G_{\mathrm{FWM}} \approx 10^6$, in agreement with the experimental observations of Ref. 3.

The obtained value in Ref. 3 for the nonlinear susceptibility in silver fractal composites is $\bar{\chi}^{(3c)} \sim p \times 10^{-5}$ esu at $\lambda = 532$ nm. Even for a very small metal fraction used in the experiment of Ref. 3, $p \sim 10^{-5}$, this gives $\bar{\chi}^{(3c)} \sim 10^{-10}$ esu (cf., a typical value of $\chi^{(3)}$ in crystals is $\sim 10^{-15}$ esu). Moreover, p is a variable quantity and can be, of course, increased. We can assigned the value 10^{-5} esu to the nonlinear susceptibility, $\chi^{(3c)}$, of silver fractal clusters; the quantity $\chi^{(3c)}$ is related to the nonlinear susceptibility, $\bar{\chi}^{(3c)}$, of the composite (silver aggregates in water) via the relation $\bar{\chi}^{(3c)} = p \times \chi^{(3c)}$. The huge nonlinearity, $\chi^{(3c)} \sim 10^{-5}$ esu, with a time of the nonlinear response $\leqslant 30$ ps,[3] makes metal fractal aggregates very interesting for potential applications.

In the long-wavelength range of the spectrum, $\lambda > 1000$ nm, the quantity X is almost constant: $X(\lambda) \approx X_0$, where $a^3 X_0 = -4\pi/3$ (i.e., $X_0 = -4\pi/3$ in $a=1$ units). The excitation in this spectral region, when $X(\lambda) \approx X_0$ for all λ, can be described in terms of the single mode, called "zero mode" (see Sec. V the preceding paper, Ref. 20). In this case, all the spectral dependence for G_{FWM} is due to a λ dependence of the factor δ^{-6} in (36). Since $G_{\mathrm{FWM}} \sim |\bar{\chi}^{(3c)} v_0 / \beta^{(3)}|^2$, we conclude that $\bar{\chi}^{(3c)} \propto \delta^{-3}$ in the long-wavelength part of the spectrum. According to formulas (21) and (23) of the preceding paper,[20] for the Drude model, $\delta \propto \lambda$ in the infrared part of the spectrum; thus, $\bar{\chi}^{(3c)}$ strongly increases towards the longer wavelengths, $\propto \lambda^3$.

B. Enhanced harmonic generation

We consider now harmonic generation and begin with third-harmonic generation (THG). We assume that the phase-matching condition is fulfilled. The THG process is due to a third-order nonlinearity. The corresponding nonlinear dipole moment is

$$d_{i,\alpha}^{\mathrm{NL}} = \beta^{(3)}_{\alpha\beta\gamma\delta} E_{i,\beta} E_{i,\gamma} E_{i,\delta}. \tag{37}$$

For isotropic media, the orientation-average nonlinear polarizability may be expressed in terms of one independent constant[28]

$$\langle \beta^{(3)}_{\alpha\beta\gamma\delta}(-3\omega;\omega,\omega,\omega)\rangle_0 = f \Delta^{+}_{\alpha\beta\gamma\delta}. \tag{38}$$

We first assume that the generated signal $\omega_s = 3\omega$ lies outside the cluster band of resonant modes and, therefore, neglect the interaction of nonlinear dipoles oscillating at the frequency ω_s [cf., Eqs. (10) and (37)].

Similarly as done to obtain (13) from (10), we substitute (2) for the local fields in (37) and factorize the average over the orientations and over an ensemble of random clusters. This gives the following expression for the nonlinear polarizability of a particle in a cluster:

$$\langle \beta^{(3c)}_{\alpha\beta\gamma\delta}\rangle = Z^3 \langle \beta^{(3)}_{\alpha\beta'\gamma'\delta'}\rangle_0 \langle \alpha_{j,\beta'\beta} \alpha_{j,\gamma'\gamma} \alpha_{j,\delta'\delta}\rangle. \tag{39}$$

Further, similarly to the method used to obtain (16)–(18) from (13), we find

$$\langle \beta^{(3c)}_{\alpha\beta\gamma\delta}\rangle = F \Delta^{+}_{\alpha\beta\gamma\delta}, \tag{40}$$

where

$$F = \frac{1}{15} Z^3 f_s \langle \mathrm{Tr}(\hat{\alpha}_i)\mathrm{Tr}(\hat{\alpha}_i^T \hat{\alpha}_i) + 2\,\mathrm{Tr}(\hat{\alpha}_i \hat{\alpha}_i^T \hat{\alpha}_i)\rangle. \tag{41}$$

Note that the cluster polarizability, $\langle \beta^{(3c)}_{\alpha\beta\gamma\delta}\rangle$, is totally symmetric as well as the polarizability of an isolated monomer, $\langle \beta^{(3)}_{\alpha\beta\gamma\delta}\rangle_0$; either is characterized by a single amplitude.

Enhancement of the third-harmonic generation process is given by $G_{\mathrm{THG}} = |\langle F/f\rangle|^2$; using (41), this results in

$$G_{\mathrm{THG}} = \frac{(X^2+\delta^2)^3}{225} |\langle \mathrm{Tr}(\hat{\alpha}_i)\mathrm{Tr}(\hat{\alpha}_i^T \hat{\alpha}_i) + 2\,\mathrm{Tr}(\hat{\alpha}_i \hat{\alpha}_i^T \hat{\alpha}_i)\rangle|^2. \tag{42}$$

For the excitation outside the cluster band of resonant modes, $\alpha_i \approx \alpha_0$ and $G_{\mathrm{THG}} = 1$ in (42).

In Fig. 3, we present a log-log plot of G_{THG} as a function of X for three very different values of δ. Despite the strong fluctuations, we can conclude from Fig. 3 that, on average, the product $G_{\mathrm{THG}}\delta^4$ does not depend on δ. Thus, in contrast to the binary theory,[2] that predicts a small enhancement for the highest-order harmonic generation, the present calculations demonstrate a possibility of a very strong enhancement: $G_{\mathrm{THG}} \propto \delta^{-4}$.

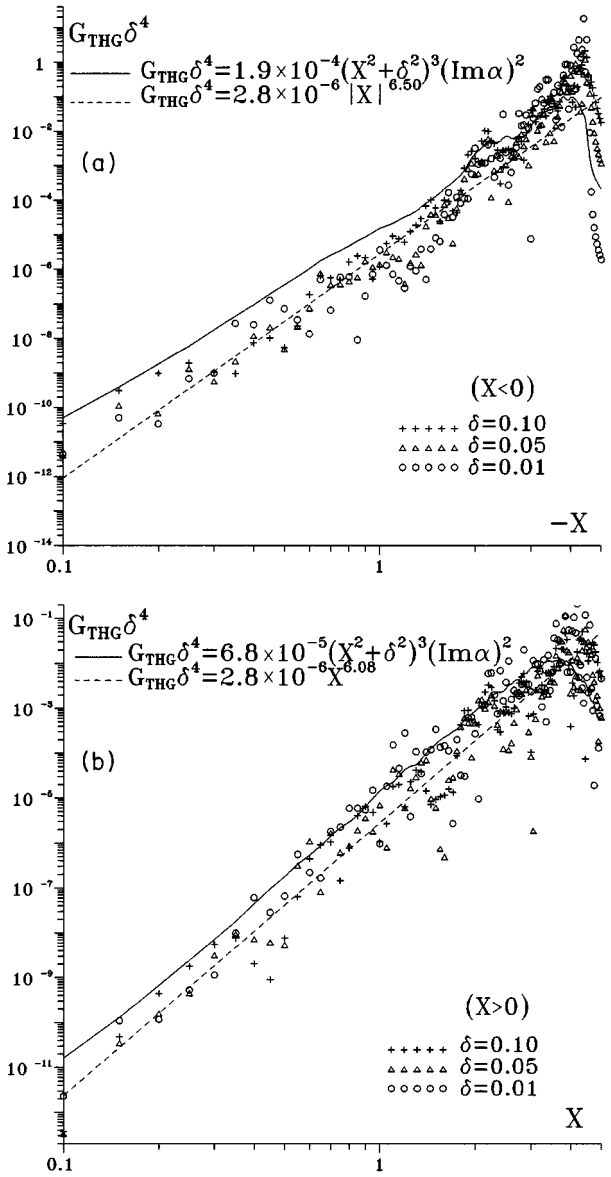

FIG. 3. The enhancement of the third-harmonic generation, G_{THG}, in CCA's for negative (a) and positive (b) X. See also the text.

Based on the results of our simulations, we suggest the following expression for the enhancement factor within a band of the eigenmodes:

$$G_{\mathrm{THG}}\approx C_{\mathrm{THG}}\frac{(X^2+\delta^2)^3}{\delta^4}[\mathrm{Im}\alpha(X)]^2, \tag{43}$$

where the prefactor, C_{THG}, is an adjustable parameter. Formula (43) reflects, in particular, the indicated dependence $G_{\mathrm{THG}}\propto\delta^{-4}$.

The solid lines in Fig. 3 represent the results of calculations using (43) with C_{THG} found from the different relations for positive and negative X: $G_{\mathrm{THG}}\delta^4=0.1$ in its maximum (at $X\approx-4$) for negative X, and $G_{\mathrm{THG}}\delta^4=0.01$ in its maximum (at $X\approx4$) for positive X. Recall that for FWM the value of C_{FWM} was chosen so that $G_{\mathrm{FWM}}\delta^6=1$ in both of its maxima at $X\approx\pm4$. Thus, in order to fit the simulations, we have to take the smaller values for the product $G_{\mathrm{THG}}\delta^4$ in its maxima. This is probably due to the fact that the product of the α_i in (41) has poles (as a function of w_n) lying in the same complex semiplane; therefore, the average enhancement, which can be estimated by integrating over w_n, is smaller. [In contrast, there is a complex conjugate term, α_i^*, in the product of the α_i in expression (25) that defines the enhancement for FWM. Note that the presence of α_i^* $\propto E_i^*$ in the nonlinear response indicates that an elementary quantum mechanical process includes "subtraction" of a photon.] Despite the indicated difference, the enhancement, G_{THG}, is very large and can reach giant values for small values of δ.

The dashed lines in Fig. 3. show a power-law fit for $0.1\leqslant|X|\leqslant3$ ($\delta=0.05$). The computed exponents are 6.08 ± 1.00 for $X>0$ and 6.5 ± 1.0 for $X<0$. However, the fluctuations are so strong that based on the simulations we cannot claim that there is a pronounced power-law dependence.

In general, enhancement of nth-harmonic generation may be estimated by

$$G_{n\mathrm{HG}}\sim\left|\left\langle\frac{E_i^n}{[E^{(0)}]^n}\right\rangle\right|^2\sim|\alpha_0|^{-2n}|\langle\alpha_i^n\rangle|^2. \tag{44}$$

The estimate (44) is based on the assumption that the interaction of nonlinear dipoles oscillating at the frequency $\omega_s=n\omega$ can be ignored. If this interaction is of importance, the estimate (44) should be replaced by

$$G_{n\mathrm{HG}}\sim|\alpha_0(\omega)|^{-2n}|\alpha_0(\omega_s)|^{-2}|\langle\alpha_i^n(\omega)\alpha_i(\omega_s)\rangle|^2. \tag{45}$$

The experimental observation of the enhanced (by 3 orders of magnitude) second-harmonic generation was reported in Ref. 29.

C. Enhanced Raman scattering

In this section we consider the enhancement of Raman scattering, G_{RS}, in particles aggregated into clusters. In our previous work on this subject,[22] the simulations of the enhancement were performed only for diluted cluster-cluster aggregates, whereas below we calculate G_{RS} for nondiluted CCA's and compare the results with experimental observations.

We assume that each monomer of a cluster, apart from the linear polarizability, α_0, possesses also a Raman polarizability, κ. This means that the exciting field, $\mathbf{E}^{(0)}$, applied to an isolated monomer, induces a dipole moment, $\mathbf{d}^s$, oscillating at the Stokes-shifted frequency, ω_s. To avoid unessential complications, we suppose κ to be a scalar; this gives $\mathbf{d}^s=\kappa\mathbf{E}$. The Raman polarizability may be either due to the polarizability of a monomer itself or to an impurity bound to the monomer.

We consider spontaneous Raman scattering, which is an incoherent optical process. This means that the Raman polarizabilities, κ_i, of different monomers possess uncorrelated random phases:

$$\langle\kappa_i^*\kappa_j\rangle=|\kappa|^2\delta_{ij}. \tag{46}$$

This feature constitutes the principal distinction between κ and the linear polarizability, α. It ensures that there exists no interference of the Stokes waves generated by different monomers.

As was pointed out above, the field acting upon an ith monomer in a cluster is the local field, $\mathbf{E}_i$, rather than the external field, $\mathbf{E}^{(0)}$. Also, the dipole interaction of monomers at the Stokes-shifted frequency, ω_s, should be included. Taking these arguments into account, we write the following system of equations:

$$d^s_{i\alpha}=\kappa_i E_{i\alpha}+\alpha^s_0\sum_j\ (i\alpha|W|j\beta)d^s_{j\beta}, \tag{47}$$

where α^s_0 is the linear polarizability of an isolated monomer at the Stokes-shifted frequency, ω_s.

The total Stokes dipole moment, $\mathbf{D}^s$, found by solving (47), is:[22]

$$D^s_\alpha=\sum_i\ d^s_{i\alpha}=Z_sZ\sum_j\ \kappa_j\alpha^s_{j,\beta\alpha}\alpha_{j,\beta\beta'}E^{(0)}_{\beta'}, \tag{48}$$

where $Z_s=(\alpha^s_0)^{-1}$, $\alpha^s_i\equiv\alpha_i(X_s)$, and α_i is defined in (3).

The RS enhancement associated with particle clustering is defined as[22]

$$G_{\rm RS}=\frac{\langle|\mathbf{D}_s|^2\rangle}{N|\kappa|^2|\mathbf{E}^{(0)}|^2}. \tag{49}$$

The above formulas (47)–(49) are exact and valid for any cluster of particles. If the Stokes shift is so large that the Raman-scattered light is well out of the absorption band of the cluster, the polarizability α^s_i in (48) and (49) can be approximated as $\alpha^s_{i,\alpha\beta}\approx Z_s^{-1}\delta_{\alpha\beta}$, and the orientation-average enhancement (49) acquires the following form:[22]

$$G_{\rm RS}=|Z|^2\frac{1}{3N}\left\langle\sum_i\ |\alpha_{i,\alpha\beta}|^2\right\rangle=\delta(1+X^2/\delta^2){\rm Im}\alpha. \tag{50}$$

Thus, if the Raman-scattered light does not interact with the cluster, the Raman-scattering intensity is simply proportional to the mean square of the local fields, $G_{\rm RS}=G$ [cf. Eq. (5)].[22]

However, in more interesting case, the Stokes shift is small and the Stokes amplitudes are also enhanced. Then, the general expression (49) is needed; after averaging over orientations, this gives

$$G_{\rm RS}=\frac{(X^2+\delta^2)^2}{3}\langle{\rm Tr}[\hat\alpha^T_i\hat\alpha_i\hat\alpha^{T*}_i\hat\alpha^*_i]\rangle. \tag{51}$$

[For the nonresonant case, $|X|\gg|w_n|$, we have $\alpha_i=\alpha_0$ and, therefore, $G_{\rm RS}=1$ in Eq. (51).] According to (51), the enhancement of Raman scattering is determined by the enhanced local fields raised to the fourth power and averaged over an ensemble of clusters,

$$G_{\rm RS}\sim\langle|E_i/E^{(0)}|^4\rangle\sim|\alpha_0^{-1}|^4\langle|\alpha_i|^4\rangle. \tag{52}$$

Similar to the case of FWM [see (26)–(30)], we may express the RS enhancement in the form

$$G_{\rm RS}=\frac{(X^2+\delta^2)^2}{3}\langle g_{\rm RS}(X)\rangle, \tag{53}$$

with $g_{\rm RS}(X)$ given by

$$g_{\rm RS}\equiv{\rm Tr}[\hat\alpha^T_i\hat\alpha_i\hat\alpha^{T*}_i\hat\alpha^*_i]$$

$$=\sum_{nmlk}K_{nmlk}\Lambda_n\Lambda_m\Lambda^*_l\Lambda^*_k, \tag{54}$$

where K_{nmlk} is defined in (29).

The function $g_{\rm RS}$ satisfies the following sum rule:[22]

$$\int_{-\infty}^{\infty}g_{\rm RS}(X)dX=4\pi\ {\rm Im}\sum_{nmlk}K_{nmlk}R_{nk}R_{ml}R_{nl}. \tag{55}$$

Further, similar to (33), the product of the Λ factors in Eq. (54) can be rewritten as

$$\Lambda_n\Lambda_m\Lambda^*_l\Lambda^*_k=R_{ml}R_{nk}\{(\Lambda_n\Lambda_m+\Lambda^*_l\Lambda^*_k)-R_{nl}(\Lambda_n-\Lambda^*_l)$$
$$-R_{mk}(\Lambda_m-\Lambda^*_k)\}. \tag{56}$$

We first find $g^r_{\rm RS}(X)$ due to the ''resonant'' difference of the eigenmodes only, such that $|w_n-w_m|\ll\delta$ in (54). In this case, for the ensemble average, we obtain

$$\langle g^r_{\rm RS}(X)\rangle=\frac{3}{2\delta^3}\,{\rm Im}\alpha(X). \tag{57}$$

The sum rule for the ensemble-average resonant contribution has the form

$$\int_{-\infty}^{\infty}\langle g^r_{\rm RS}(X)\rangle dX=\frac{3\pi}{2\delta^3}. \tag{58}$$

It was shown in Ref. 22 that the resonant factor $\langle g^r_{\rm RS}(X)\rangle$ gives the dominant contribution to the enhancement for diluted clusters. We conjecture that $\langle g^r_{\rm RS}(X)\rangle$ describes the functional dependence of the enhancement on X and δ for nondiluted clusters as well:

$$G_{\rm RS}\approx C_{\rm RS}\frac{(X^2+\delta^2)^2}{\delta^3}{\rm Im}\alpha(X), \tag{59}$$

with $C_{\rm RS}$ being an adjustable parameter.

In Fig. 4, we plot the results of our simulations of $G_{\rm RS}$ defined in (51) for negative (a) and positive (b) values of X. The solid lines in Fig. 4 give the enhancement found from (59), with $C_{\rm RS}$ obtained from the relation: $G_{\rm RS}\delta^3=3$ in the maxima occurring at $X\approx\pm4$. The dashed lines represent a power-law fit for $G_{\rm RS}\delta^3$ in the interval $0.1\leqslant|X|\leqslant3$, with $\delta=0.05$. The obtained power exponents (4.07 ± 0.70 for $X<0$ and 4.01 ± 0.70 for $X>0$) are close to 4 for both positive and negative values of X. Similar to the above-considered cases [see the discussion following Eq. (36)], the dependence X^4 in (59) dominates the weak spectral dependence of ${\rm Im}\alpha(X)$ in the band of cluster modes.

As seen in Fig. 4, the product $G_{\rm RS}\delta^3$, on average, does not depend on δ in the region close to the maxima, and its value there is close to unity. Thus, the strong enhancement of Raman scattering, $G_{\rm RS}\sim\delta^{-3}$, can be obtained due to aggregation of particles into fractal clusters.

In Fig. 5, experimental RS enhancement data, obtained for a silver colloid solution in Ref. 30, are compared with

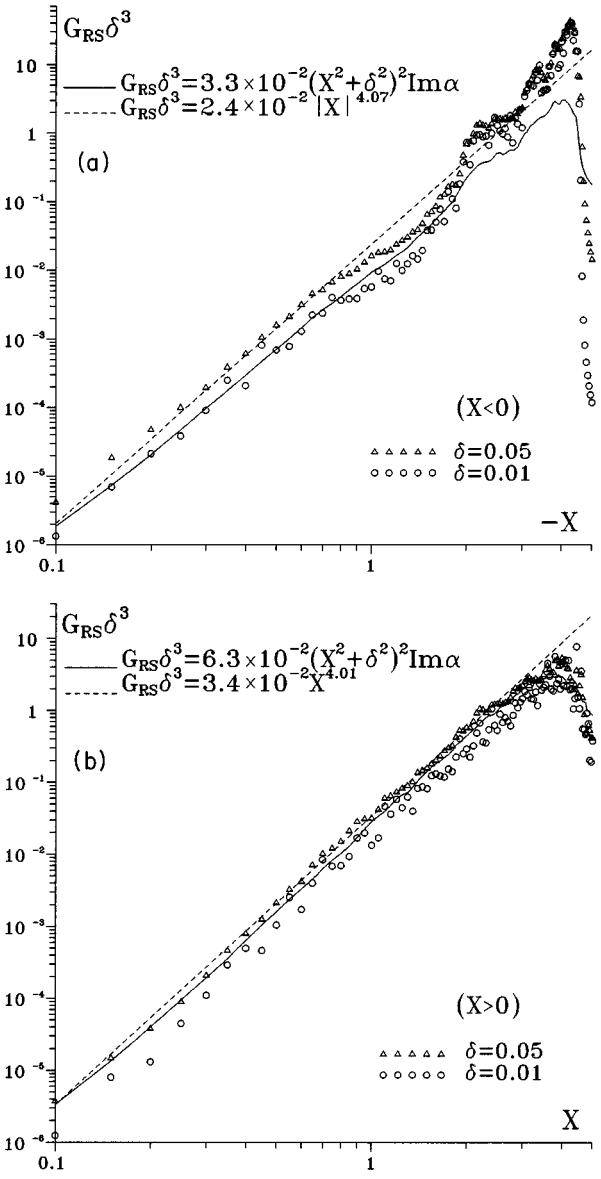

FIG. 4. The enhancement of Raman scattering in CCA's, G_{RS}, for negative (a) and positive (b) X. For details, see the text.

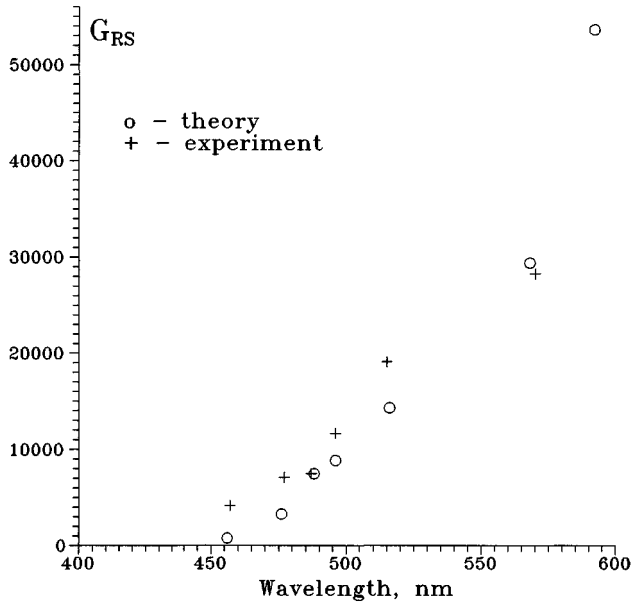

FIG. 5. Theoretical and experimental enhancement factors, G_{RS}, for the silver colloid aggregates as a function of wavelength, λ.

G_{RS} calculated using (51). [The values of X and δ for various λ were found using (21) and (22) of Ref. 20 and the data of Ref. 26.] Only the spectral dependence of G_{RS} is informative in this figure since only relative values of G_{RS} are reported in Ref. 30. The experimental data presented in Fig. 5 are normalized by setting $G_{\mathrm{RS}}\simeq3\times10^4$ at 570 nm, which is a reasonable value. Clearly, the present theory successfully explains the giant enhancement accompanying particle aggregation and the observed increase of G_{RS} towards the red part of the spectrum. (The agreement is better than that obtained with the use of the model of diluted clusters.[22]) The strong enhancement towards the red occurs because the local fields associated with collective dipolar modes in CCA's become significantly larger in the red part of the spectrum (see Fig. 1).

D. Nonlinear refraction and absorption

In this section we consider the enhancement of the optical Kerr nonlinearity. The Kerr polarizability has, in general, the form $\beta^{(3)}_{\alpha\beta\gamma\delta}(\omega;\omega,\omega,-\omega)$, and determines nonlinear corrections ($\propto$ the field intensity) to the refractive index and absorption. The Kerr-type nonlinearity can also result in degenerate four-wave mixing (DFWM) considered above. Composite materials with large values of the Kerr nonlinearity can be used as nonlinear optical filters. Under certain conditions, they also manifest optical bistability[14] which can be utilized to build an optical analog of the electric transistor. Therefore, there is significant interest in developing materials with a large Kerr nonlinearity.

We consider the enhancement of the Kerr susceptibility due to the clustering of small particles embedded in a linear host material. We assume that the volume fraction, p, filled by particles is small, and they are initially randomly distributed in the host. Since p is small, the interaction between nonaggregated particles is negligible. The aggregation results in many well-separated random clusters. The interactions between the dipoles induced by light on particles in a cluster lead to the formation of collective eigenmodes; their resonant excitation results in high local fields and the enhanced Kerr susceptibility.

The Kerr nonlinear polarizability, $\beta^{(3)}$, has the same structure [see Eq. (6)] as the one describing DFWM. (In the present case, however, we assume that there is only one applied field, $\mathbf{E}^{(0)}$.) Although in Sec. III A we considered only one specific process, DFWM, the analysis presented there was general and most of the obtained results are applicable for other phenomena associated with the Kerr susceptibility.

For isotropic media, the Kerr polarizability can be written in the form (7), with two independent constants, f_s and f_a, that are related to the constants a and b in formulas (19) and (20). The polarization of a composite with aggregated particles can be presented as follows:

$$P^{(3c)}_{\alpha}(\omega)=3\overline{\chi}^{(3c)}_{\alpha\beta\gamma\delta}(-\omega;\omega,\omega,-\omega)E^{(0)}_{\beta}E^{(0)}_{\gamma}E^{(0)*}_{\delta},$$

where the effective Kerr susceptibility, $\bar{\chi}^{(3c)}$, of the composite has the form [cf. (13) and (23)]

$$\bar{\chi}^{(3c)}_{\alpha\beta\gamma\delta}=pZ^3Z^*\langle\chi^{(3)}_{\alpha'\beta'\gamma'\delta'}\rangle_0\langle\alpha_{j,\alpha'\alpha}\alpha_{j,\beta'\beta}\alpha_{j,\gamma'\gamma}\alpha^*_{j,\delta'\delta}\rangle, \tag{60}$$

and $\langle\chi^{(3)}_{\alpha\beta\gamma\delta}\rangle_0=v_0^{-1}\langle\beta^{(3)}_{\alpha\beta\gamma\delta}\rangle_0$, with v_0 being the volume of a particle.

Proceeding similarly to the method that was used to obtain (16)–(18) from (13), we find

$$\bar{\chi}^{(3c)}_{\alpha\beta\gamma\delta}=G_{K,s}p\phi_s\Delta^+_{\alpha\beta\gamma\delta}+G_{K,a}p\phi_a\Delta^-_{\alpha\beta\gamma\delta}, \tag{61}$$

where $\phi_{s,a}=v_0^{-1}f_{s,a}$,

$$G_{K,s}=\frac{1}{15}Z^3Z^*\langle\mathrm{Tr}(\hat{\alpha}_i^T\hat{\alpha}_i)\mathrm{Tr}(\hat{\alpha}_i^T\hat{\alpha}_i^*)+2\,\mathrm{Tr}(\hat{\alpha}_i^T\hat{\alpha}_i\hat{\alpha}_i^T\hat{\alpha}_i^*)\rangle, \tag{62}$$

and

$$G_{K,a}=\frac{1}{6}Z^3Z^*\langle\mathrm{Tr}(\hat{\alpha}_i^T\hat{\alpha}_i)\mathrm{Tr}(\hat{\alpha}_i^T\hat{\alpha}_i^*)-\mathrm{Tr}(\hat{\alpha}_i^T\hat{\alpha}_i\hat{\alpha}_i^T\hat{\alpha}_i^*)\rangle. \tag{63}$$

The factors G_s and G_a are identical to F_s/f_s and F_a/f_a, respectively [see Eqs. (17) and (18)], and the enhancement for the DFWM process can be expressed in terms of $G_{K,s}$ as $G_{\mathrm{FWM}}=|G_{K,s}|^2$.

In general, according to (61)–(63), there are two different enhancement coefficients for totally symmetric ($\propto\Delta^+_{\alpha\beta\gamma\delta}$) and partially symmetric ($\propto\Delta^-_{\alpha\beta\gamma\delta}$) parts of the susceptibility in an isotropic system.[31] The fact that there are two different independent constants for the Kerr response in an isotropic medium results, in particular, in a rotation of the polarization ellipse.[28] If the field $\mathbf{E}^{(0)}$ is polarized linearly or circularly, the nonlinear polarization, $\mathbf{P}^{(3c)}$, can be expressed in terms of only one independent constant (F_s and $[F_s+F_a]$ for linear and circular polarization, respectively).[28] Also, in the low-frequency limit (where $\beta^{(3)}$ is due to the nonresonant electron response), the nonlinear susceptibility tensor must be fully symmetrical, i.e., $F_a=0$, for an arbitrary light polarization.[28] Below, we calculate the enhancement associated with $G_{K,s}\equiv G_K$. The enhancement factor is, in general, complex: $G_K\equiv G'_K+iG''_K$. If $\beta^{(3)}$ is real, the real part, G'_K, and the imaginary part, G''_K, determine the enhancement for the nonlinear refraction and for the nonlinear correction to absorption, respectively.

The enhancement for Kerr media can be also presented in the form

$$G_K=\frac{(X^2+\delta^2)(X+i\delta)^2}{15}\langle g_K\rangle, \tag{64}$$

where $g_K\equiv g_{\mathrm{FWM}}$, and g_{FWM} is defined in (26)–(29). It was conjectured in Sec. III A that $\langle g_{\mathrm{FWM}}\rangle$ and G_{FWM} can be expressed in terms of the absorption $\mathrm{Im}\alpha(X)$ [see Eqs. (34) and (36)]. Accordingly, we assume that G'_K is larger than G''_K [so that $g_{\mathrm{FWM}}\equiv g_K$ can be approximately considered as a real quantity, in agreement with (34)]; then for $|X|\gg\delta$, we obtain

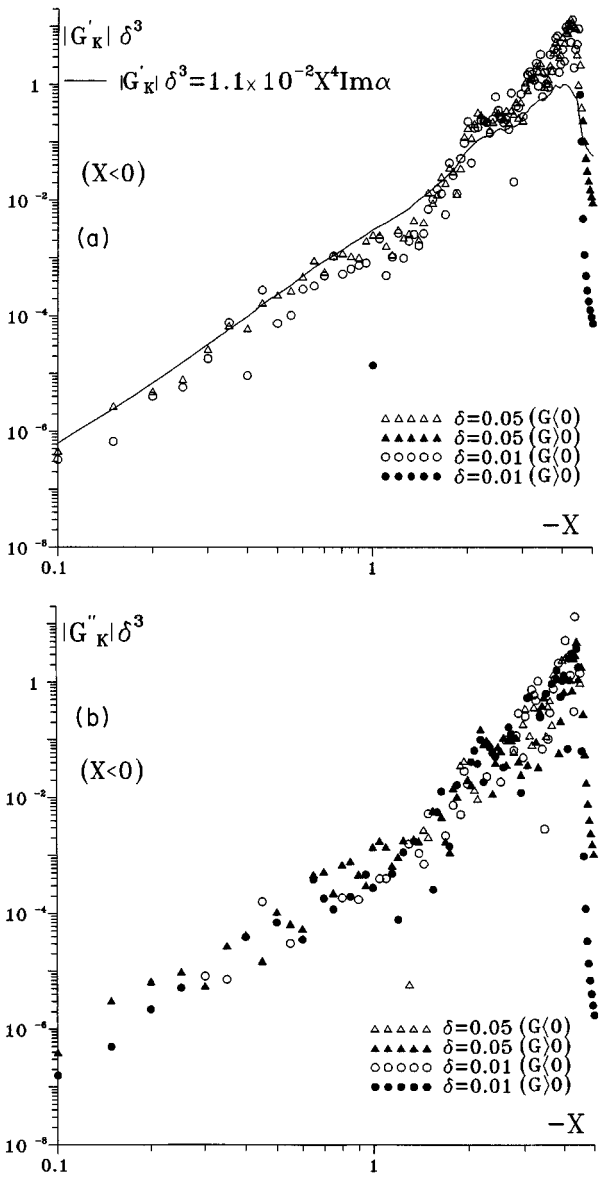

FIG. 6. The enhancement of the Kerr optical susceptibility in CCA's: (a) the real part, G'_K, and (b) the imaginary part, G''_K.

$$G'_K\approx C_K\frac{X^4}{\delta^3}\,\mathrm{Im}\alpha(X). \tag{65}$$

In Fig. 6, we present plots of G'_K (a) and G''_K (b) for $X<0$ (the calculations for $X>0$ give similar results). The solid line in Fig. 6(a) represents the calculations based on Eq. (65), with the C_K chosen so that $|G'_K\delta^3|=1$ in its maxima at $X\approx-4$. From the figure, we can conclude that Eq. (65) approximates the exact results well. Also, as follows from the figure, both real and imaginary parts of the enhancement are approximately proportional to the third power of the quality factor, $q^3(\sim\delta^{-3})$, and the following estimates are valid in the maxima: $G'_K\delta^3\sim1$ and $G''_K\delta^3\sim1$ (actually, G'_K is several times larger than G''_K, in accordance with the above assumption). For metal particles, in particular, the decay parameter varies from $\delta=0.01$ to $\delta=0.1$ in the infrared and visible parts of the spectrum; accordingly, the enhancement ranges from $|G_K|\sim10^3$ to $|G_K|\sim10^6$ in this spectral range. Such a

giant enhancement indicates that optical materials based on composites including small-particle clusters possess a high potential for various applications.

It also follows from the figures that, in accordance with (34) and (64), the real part G_K' is negative for most of the resonant modes, and $|G_K'|$ statistically dominates $|G_K''|$. For $G_K'<0$, the nonlinear correction to the refractive index, Δn, is negative, if $\beta^{(3c)}>0$, and positive, if $\beta^{(3c)}<0$ (leading to self-defocusing and self-focusing of the light beam, respectively). Interestingly, the imaginary part G_K'', changes its sign as a function of X very rapidly. Thus, a nonlinear correction to the absorption coefficient (given by G_K'' for real $\beta^{(3c)}$) is a very strong function of the laser frequency and can be both positive and negative. The fact that the nonlinear contribution to the absorption can have a different sign is not surprising: there are nonlinear optical processes (associated with the Kerr-type nonlinearity) leading to both positive and negative nonlinear contributions to absorption. In particular, processes, such as the saturation effect or the Rayleigh resonance, lead to negative corrections to absorption, whereas two-photon absorption, for example, results in a positive correction.[28] Clearly, the light excites simultaneously many resonant and quasiresonant modes in a cluster, leading to a competition between the contributions associated with various optical processes; this probably results in the strong dependence of G_K'' on X.

IV. CONCLUDING REMARKS

As shown above, the clustering of small particles embedded in a host material may result in a giant enhancement of both linear (e.g., Raman scattering) and nonlinear (four-wave mixing, harmonic generation, and nonlinear reflection and absorption) optical effects. The enhancement occurs because of strongly fluctuating local fields that can have very large values in particle aggregates (see Fig. 1). Nonlinearities emphasize these fluctuations leading to giant enhancements.

If particles aggregate into fractal clusters, fluctuations of the local fields are especially large. This is because the dipole interactions in fractals are not long range (as they are in conventional three-dimensional media) and many of the collective eigenmodes are strongly localized in different parts of a cluster with various random structures. This ultimately leads to strong spatial fluctuations of the fields. In contrast, in compact three-dimensional clusters of particles, the long-range dipolar interaction involves all particles into the excitation, thereby suppressing fluctuations (see Fig. 1).

Enhancements in small-particle clusters can be understood and roughly estimated using the following simple arguments. Consider the enhancement for an arbitrary nonlinear optical process $\propto E^n$. According to Eqs. (2) and (3), for the resonant dipolar eigenmodes, the local fields, E_i, exceed the external field, $E^{(0)}$, by the factor $\sim|\alpha_0^{-1}/\delta| = |X+i\delta|/\delta$, i.e., $\sim|X|/\delta$ for $|X|\gg\delta$. However, the fraction of the monomers involved in the resonant optical excitation is small, $\sim\delta\mathrm{Im}\alpha(X)$.

For a nonlinear optical process, $\propto|E|^n$, one can estimate the ensemble average of the enhancement, $\langle|E_i/E^{(0)}|^n\rangle$, as the resonant value, $|E_i/E^{(0)}|^n_{\mathrm{res}}$, multiplied by the fraction of the resonant modes (in other words, the fraction of particles involved in the resonant excitation). This gives, for the enhancement the following estimate,

$$\langle|E_i/E^{(0)}|^n\rangle\sim|X|^n\delta^{-n}\times\delta\,\mathrm{Im}\alpha(X)\sim|X|^n\delta^{1-n}\mathrm{Im}\alpha(X), \tag{66}$$

which is $\gg 1$ for $n>1$. Since this is only a rough estimation, an adjustable constant, C, should be, in general, added as a prefactor.

The nonlinear dipole amplitude can be enhanced along with the linear local fields provided the generated frequency lies within the spectral region of the cluster eigenmodes. For enhancements of incoherent processes, such as Raman scattering and nonlinear refraction and absorption in Kerr media, we obtain from Eq. (66): $G\sim CX^4\delta^{-3}\mathrm{Im}\alpha(X)$ [cf. (59) and (65)]. For coherent processes, the resultant enhancement $\sim|\langle|E_i/E^{(0)}|^n\rangle|^2$; accordingly, the enhancement factor $\sim CX^6\delta^{-4}[\mathrm{Im}\alpha(X)]^2$ for the third-harmonic generation [cf. Eq. (43)], and $\sim CX^8\delta^{-6}[\mathrm{Im}\alpha(X)]^2$ for degenerate four-wave mixing [cf. (36)]. (The latter enhancement is larger because of the ''additional'' enhancement of the generated nonlinear amplitudes oscillating at the same frequency as the applied field.)

There are other optical phenomena (not considered here) that can be also enhanced in small-particle composites. For example, Rayleigh scattering is enhanced by the factor $G_R\sim\langle|E_i/E^{(0)}|^2\rangle\propto\delta^{-1}$.[21] Another example is fluorescence from molecules adsorbed on a small-particle aggregate. The fluorescence following two-photon absorption by the aggregate is enhanced by the factor $G_F\sim\langle|E_i/E^{(0)}|^4\rangle \sim|\alpha_0|^{-4}\langle|\alpha_i|^4\rangle\propto\delta^{-3}$.

ACKNOWLEDGMENTS

This research was supported by NSF under Grant No. DMR-9500258 and by NATO under Grant No. CRG 950097.

*Also with the L. V. Kirensky Institute of Physics, Siberian Branch of the Russian Academy of Science, 660036 Krasnoyarsk, Russia.

†Also with the Institute of Automation and Electrometry, Siberian Branch of the Russian Academy of Science, 630090 Novosibirsk, Russia.

[1] D. Stroud and P. M. Hui, Phys. Rev. B **37**, 8719 (1988).

[2] A. V. Butenko, V. M. Shalaev, and M. I. Stockman, Z. Phys. D **10**, 81 (1988). The spectral function $S_\alpha(z)$ of Ref. 2 must be replaced by the function $S_D(z)$ of Ref. 16 that corrects the former one.

[3] S. G. Rautian, V. P. Safonov, P. A. Chubakov, V. M. Shalaev, and M. I. Stockman, Pis'ma Zh. Éksp. Teor. Fiz. **47**, 243 (1988) [JETP Lett. **47**, 243 (1988)]; A. V. Butenko *et al.*, Z. Phys. D **17**, 283 (1990).

[4] V. M. Shalaev, M. I. Stockman, and R. Botet, Physica A **185**, 181 (1992).

[5] V. M. Shalaev, V. A. Markel, and V. P. Safonov, Fractals **2**, 201 (1994); V. M. Shalaev, R. Botet, D. P. Tsai, J. Kovacs, and M. Moskovits, Physica A **207**, 197 (1994).

[6] D. J. Bergman and D. Stroud, *Physical Properties of Macroscopically Inhomogeneous Media*, Solid State Physics (Academic

Press, New York, 1992), Vol. 46, p. 147; D. J. Bergman, Phys. Rev. B **39**, 4598 (1989).

[7] C. Flytzanis, Prog. Opt. **29**, 2539 (1992); D. Ricard, Ph. Roussignol, and C. Flytzanis, Opt. Lett. **10**, 511 (1985); F. Hache, D. Ricard, C. Flytzanis, and U. Kreibig, Appl. Phys. A **47**, 347 (1988).

[8] K. W. Yu, Y. C. Wang, P. M. Hui, and G. Q. Gu, Phys. Rev. B **47**, 1782 (1993); K. W. Yu, P. M. Hui, and D. Stroud, *ibid.* **47**, 14150 (1993).

[9] J. E. Sipe and R. W. Boyd, Phys. Rev. B **46**, 1614 (1992).

[10] P. M. Hui and D. Stroud, Phys. Rev. B **49**, 11729 (1994).

[11] K. W. Yu, Phys. Rev. B **49**, 9989 (1994).

[12] D. Stroud and X. Zhang Physica A **207**, 55 (1994); X. Zhang and D. Stroud, Phys. Rev. B **49**, 944 (1994).

[13] P. M. Hui, Phys. Rev. B **49**, 15344 (1994); K. W. Yu, Y. C. Chu, and Eliza M. Y. Chan, *ibid*. **50**, 7984 (1994).

[14] O. Levy, D. J. Bergman, and D. G. Stroud, Phys. Rev. E **52**, 3184 (1995); D. Bergman, O. Levy, and D. Stroud, Phys. Rev. B **49**, 129 (1994); O. Levy and D. Bergman, Physica A **207**, 157 (1994).

[15] V. M. Shalaev and M. I. Stockman, Z. Phys. D **10**, 71 (1988).

[16] V. A. Markel, L. S. Muratov, M. I. Stockman, and T. F. George, Phys. Rev. B **43**, 8183 (1991); M. I. Stockman, L. N. Pandey, L. S. Muratov, and T. F. George, Phys. Rev. Lett. **72**, 2486 (1994); M. I. Stockman, L. N. Pandey, L. S. Muratov, and T. F. George, Phys. Rev. B **51**, (1995).

[17] V. M. Shalaev, R. Botet, and A. V. Butenko, Phys. Rev. B **48**, 6662 (1993).

[18] D. P. Tsai, J. Kovacs, Z. Wang, M. Moskovits, V. M. Shalaev, J. Suh, and R. Botet, Phys. Rev. Lett. **72**, 4149 (1994); V. M. Shalaev and M. Moskovits, *ibid*. **75**, 2451 (1995).

[19] A diluted cluster is obtained from the original by random removal of monomers and successive reduction in cluster size, such that the average distance between nearest neighbors remains the same as in the original cluster. This procedure leads to improved spatial scaling at small distances while the global fractal morphology of the cluster remains unchanged (Ref. 16).

[20] V. A. Markel, V. M. Shalaev, E. B. Stechel, W. Kim, and R. L. Armstrong, the preceding paper, Phys. Rev. B **53**, 2425 (1996).

[21] V. M. Shalaev, R. Botet, and R. Jullien, Phys. Rev. B **44**, 12216 (1991); **45**, 7592(E) (1992).

[22] M. I. Stockman, V. M. Shalaev, M. Moskovits, R. Botet, and T. F. George, Phys. Rev. B **46**, 2821 (1992).

[23] R. Jullien and R. Botet, *Aggregation and Fractal Aggregates* (World Scientific, Singapore, 1987).

[24] J. A. Creighton, in *Surface Enhanced Raman Scattering*, edited by R. K. Chang and T. E. Furtak (Plenum Press, New York, 1982); D. Weitz and M. Oliveria, Phys. Rev. Lett. **52**, 1433 (1984).

[25] J. K. Collum and R. A. Willoughby, *Lanczos Algorithm for Large Symmetric Eigenvalue Computations* (Birkhäuser, Boston, 1985), Vol. 1.

[26] P. B. Johnson and R. W. Christy, Phys. Rev. B **6**, 4370 (1972).

[27] *Handbook of Optical Constants of Solids*, edited by E. D. Palik (Academic Press, New York, 1985).

[28] R. W. Boyd, *Nonlinear Optics* (Academic Press, New York, 1992); L. D. Landau, E. M. Lifshits, and L. P. Pitaevskii, *Electrodynamics of Continuous Media*, 2nd ed. (Pergamon, Oxford, 1984).

[29] I. A. Akimov, A. V. Baranov, V. M. Dubkov, V. I. Petrov, and E. A. Sulabe, Opt. Spectrosc. **63**, 756 (1987).

[30] J. S. Suh and M. Moskovits, J. Phys. Chem. **58**, 5526 (1984).

[31] Some authors define the ratio $\langle |E^{(i)}/E^{(0)}|^4 \rangle$ as the enhancement. Although this ratio can be used to estimate the enhancement G_K by an order of magnitude, it differs from the exact result (61)–(63) and, therefore, cannot be applied for finding enhancement in the general case.